Disulfide-Linked Bovine β-Lactoglobulin Dimers Fold Slowly, Navigating a Glassy Folding Landscape†

Masanori Yagi,‡ Atsushi Kameda,‡ Kazumasa Sakurai,‡ Chiaki Nishimura,§ and Yuji Goto*,‡

Institute for Protein Research, Osaka University, and CREST, Japan Science and Technology Agency, Yamadaoka 3-2, Suita, Osaka 565-0871, Japan, and Department of Molecular Biology, The Scripps Research Institute, 10550 North Torrey Pines Road, La Jolla, California 92037

Received January 30, 2008; Revised Manuscript Received April 11, 2008

ABSTRACT: To gain insight into the folding of large proteins, we constructed a bovine β-lactoglobulin (β-lg) dimeric mutant, A34C/C121A β-lg. In the mutant, a free thiol group of wild-type β-lg at Cys121 was removed and two β-lg molecules were linked by a disulfide bridge through Cys34 created at the dimer's interface. Under strongly native conditions at low concentrations of urea, the refolding yield of A34C/C121A β-lg was low when monitored by heteronuclear NMR spectroscopy. However, under marginally native conditions, the yield improved notably, although the refolding was still slow. H−D exchange pulse labeling monitored using heteronuclear NMR spectroscopy indicated that A34C/C121A β-lg forms a folding intermediate similar to monomeric C121A β-lg in spite of its slow folding. These results indicate that the rapid formation of folding intermediates driven by local interactions occurs in a manner independent of the molecular size and that, if the non-native interactions are too strong, the kinetic trap is set, leading to a glasslike misfolded state. The results suggest the important roles of marginal stability and pathways in making the folding of large proteins possible.

Some small globular proteins fold rapidly without accumulating intermediates, suggesting that the folding reactions are intrinsically efficient without a glasslike trapped state, as represented by a smooth folding funnel (*1–4*). The characterization of such fast folding, in particular the transition state, is essential for clarifying the mechanism of rapid and efficient protein folding created through evolution (*5*). On the other hand, with an increase in size, protein folding becomes complicated and more difficult. The accumulation of intermediates is common to proteins with molecular weights of 10000−20000. While the old view of protein folding considers such intermediates to be essential to the folding process, the new view based on the fast folding of small proteins and theoretical studies suggests a negative role for these intermediates in protein folding with respect to optimizing the folding rate (*6*). As for proteins with a molecular weight of more than 20000, it is generally difficult to obtain reversible unfolding except in cases where particular mechanisms circumvent kinetic trapping, e.g., domain-separated folding as observed for immunoglobulins or the participation of special factors such as molecular chaperones. Nevertheless, such larger proteins need to be expressed, refolded, and purified in vitro to perform various kinds of biological research and applications. To improve our understanding of the mechanism of protein folding, it is important to gain further insight into the folding of proteins located at the boundary between reversible and irreversible unfolding (*7*). In particular, the structural details of the intermediates leading to kinetic trapping are obscure, because irreversible folding often produces protein aggregates, usually difficult to characterize in terms of structural detail.

We chose bovine β-lactoglobulin (β-lg)[1] (*8–13*) as a target to study the mechanism of folding located at the boundary of reversible and irreversible unfolding. β-lg, a major whey protein abundant in cow's milk, is composed of 162 residues forming a β-barrel structure with nine β-strands and one main α-helix, called a lipocalin fold (see Figure 6 below). β-lg exhibits several intriguing characteristics. It binds a variety of small hydrophobic compounds such as retinol and fatty acids in its hydrophobic cavity (*10, 14*). It forms a noncovalently associated homodimer at neutral pH but exists as a monomer at acidic pH, retaining its native structure (*14–19*). Furthermore, its folding behavior is quite absorbing. Although β-lg is a predominantly β-sheet protein, its amino acid sequence shows a high α-helical propensity according to secondary structure predictions (*20, 21*), and in fact, the refolding kinetics monitored by far-UV circular dichroism (CD) indicated the transient accumulation of intermediates with non-native α-helices (*22*). The accumulation of the non-

† This work was supported by Grants-in-Aid from the Japanese Ministry of Education, Culture, Sports, Science and Technology on Priority Areas (40153770) and by a Japan Society for the Promotion of Science (JSPS) Research Fellowship for Young Scientists to M.Y.

* To whom correspondence should be addressed: Institute for Protein Research, Osaka University, Yamadaoka 3-2, Suita, Osaka 565-0871, Japan. E-mail: ygoto@protein.osaka-u.ac.jp. Telephone: 81-6-6879-8614. Fax: 81-6-6879-8616.

‡ Osaka University.

§ The Scripps Research Institute.

[1] Abbreviations: β-lg, bovine β-lactoglobulin; A_0, proton occupancy value free from the effect of a labeling pulse; ANS, 1-anilinonaphthalene-8-sulfonic acid; CD, circular dichroism; CI2, chymotrypsin inhibitor 2; H−D, hydrogen−deuterium; HSQC, heteronuclear single-quantum coherence; NMR, nuclear magnetic resonance; NOESY, nuclear Overhauser effect correlated spectroscopy; pH*, measured pH value in D_2O solution; TOCSY, total correlation spectroscopy.

10.1021/bi8001715 CCC: $40.75
Published on Web 05/08/2008

native α-helices during refolding of β-lg has been proposed to stem from local interactions with a strong α-helical preference (*22, 23*). However, because of the nonlocal interactions formed in the subsequent refolding steps, the non-native α-helices are eventually converted to the native β-structure. This conversion, an α-helix-to-β-sheet transition, is also suggested to occur during the structural change of prion protein and some amyloidogenic processes (*24, 25*).

Hydrogen−deuterium (H−D) exchange pulse labeling combined with nuclear magnetic resonance (NMR) spectroscopy is one of the most important methods providing structural information about folding intermediates at the residue level (*26*). It has been applied to β-lg as well as other proteins (*27, 28*). The β-sheet, including strands F, G, and H and the main α-helix, showed strong protection against H−D exchange within 1.8 ms of the initiation of refolding, suggesting the early formation of nativelike β-sheets in the C-terminal region. Importantly, isolated protection for residues Ile12−Ser21 was also observed, implying the existence of the non-native α-helix in the N-terminal region. However, the detailed mechanism of folding of β-lg remains unknown.

Recently, for the NMR-based characterization of the structure and folding of β-lg, we prepared a disulfide-linked dimer (A34C β-lg) (*29, 30*). The A34C β-lg dimer at neutral pH retains the native structure while suppressing the broadening of the NMR signals caused by monomer−dimer equilibrium. In this study, we used the disulfide-linked dimer to examine the effects of increasing size on protein folding. Additionally, we deleted a free thiol group of β-lg by introducing the C121A mutation, by which the reversibility of the unfolding was expected to increase significantly (*31*). The folding kinetics of the double mutant, A34C/C121A β-lg, were examined by various methods, including H−D exchange pulse labeling monitored by NMR, revealing that, although a large molecular size lowered the folding rate and yield, the structure formed at the early stage of refolding was not affected. Intriguingly, the refolding yield decreased under strongly native conditions, i.e., low denaturant concentrations. These results give a picture of the folding of large proteins: the early formation of rough secondary and tertiary structures driven by local hydrophobic interactions independent of molecular size and the slow acquisition of peripheral structures where the balance between the stabilization of native interactions and destabilization of non-native interactions is key. Moreover, the results show that the glasslike state is formed under strongly native conditions where the kinetic barriers separating the unique native state and various non-native states are too high for the trapped species to jump over.

MATERIALS AND METHODS

Proteins. Bovine β-lg mutants were expressed using a methylotrophic yeast *Pichia pastoris* expression system (*32*). Expression of C121A β-lg was performed with the same strain that was used previously (*31*). The plasmid for A34C/C121A β-lg was constructed with the template plasmid containing the sequence of C121A β-lg (*31*) and the primers employed for construction of A34C β-lg (*18*) using the QuikChange method (Stratagene, La Jolla, CA). The resultant plasmid was introduced into *P. pastoris* for expression of A34C/C121 β-lg. ^{15}N-labeled proteins were prepared by using [^{15}N]ammonia and water (Shoko Tsusho, Tokyo, Japan) to adjust the pH of the culture medium. Purification procedures were almost the same as those used previously (*30, 31*) except for the use of a HiPrep 26/60 Sephacryl S-100 HR column (GE Healthcare Life Sciences) equilibrated with 50 mM sodium phosphate and 150 mM NaCl buffer (pH 7.0) with an ÄKTAprime system (GE Healthcare Life Sciences) to remove oligomers other than dimers in the last stage of the purification of A34C/C121A β-lg. The protein concentrations were determined from the absorbance at 280 nm with molar extinction coefficients calculated from amino acid sequences as described previously (*33*).

CD Spectroscopy. CD spectra were recorded with a model 400 CD spectrometer (Aviv Biomedical, Lakewood, NJ) at 20 °C. Each sample was prepared in 20 mM glycine-HCl buffer (pH 3.0) or 20 mM sodium acetate buffer (pH 6.0) and contained each protein at 0.1 mg/mL for far-UV measurements using a 0.2 cm cell and at 0.7 mg/mL for near-UV measurements using a 1.0 cm cell. The data were represented as the mean residue ellipticity, [θ].

NMR Chemical Shift Assignments. NMR measurements for the chemical shift assignments were carried out using a DRX 600 instrument (Bruker BioSpin, Rheinstetten, Germany) at 40 °C. Each sample was prepared at a protein concentration of 9.2 mg/mL and adjusted to pH 2.5 with HCl. D_2O (10%, v/v) was added for the signal lock. Three-dimensional (3D) ^{15}N-edited TOCSY-HSQC and NOESY-HSQC spectra were used for the chemical shift assignments for C121A and A34C/C121A β-lgs. All the NMR data were processed and analyzed with NMRPipe (*34*) and Sparky (*35*). The assignments of the cross-peaks in the ^{1}H−^{15}N HSQC spectra at 30 °C were accomplished by comparison of the ^{1}H−^{15}N HSQC spectra measured at 30, 35, and 40 °C and 3D ^{15}N-edited TOCSY-HSQC spectra measured at 30 and 40 °C.

Reversibility from the Unfolded State Monitored by NMR. The nonlabeled or ^{15}N-labeled samples refolded in various urea concentrations at 20 °C were concentrated by Centriprep or Centriplus centrifugal filter units (Millipore Corp., Billerica, MA) and then buffer-exchanged using PD-10 desalting columns (GE Healthcare Life Sciences) equilibrated with dilute HCl at pH 2.5. Further concentration was performed with Centricon centrifugal filter units (GE Healthcare Life Sciences). The final protein concentration and solution volume of a sample were 5−7 mg/mL and 225 μL, respectively. D_2O (10%, v/v) was added to the sample, and the NMR measurements were taken with a Shigemi tube (Shigemi, Tokyo, Japan) using a DRX 600 instrument at 30 °C. In the case of C121A β-lg, 10 min after refolding, the samples were concentrated and buffer-exchanged to dilute HCl at pH 2.5. On the other hand, the samples of A34C/C121A β-lg were incubated for 4 h after the initiation of refolding and then concentrated. The subsequent buffer exchange was carried out 6 h after the initiation of refolding.

The chemical shift difference, $\Delta\delta$, between the native and refolded samples of A34C/C121A β-lg was calculated from the following equation

$$\Delta\delta = \sqrt{\Delta\delta_{H^N}{}^2 + (\Delta\delta_N/8)^2} \quad (1)$$

where $\Delta\delta_{H^N}$ and $\Delta\delta_N$ are the chemical shift differences in H^N and N axes, respectively.

H−D Exchange Pulse Labeling. The quench-flow pH pulse labeling experiments were performed at 20 °C with an SFM-400/QS instrument (Bio-Logic, Claix, France). The samples containing 2.3 mg/mL protein in the presence of 7.0 M urea and 20 mM glycine-HCl (pH* 2.6) in D_2O were incubated overnight in advance of the labeling to substitute all the amide protons with deuterium. Here, pH* is the measured pH value in D_2O solution. Refolding was initiated by an 8.5-fold dilution into a refolding buffer in H_2O at pH 3.0. After a refolding time of 10 ms, to accelerate H−D exchange reactions, the pH of the solution was increased to 10.0 by mixing with an alkaline buffer. The duration of the labeling pulses was 10, 13, 26, 37, and 48 ms.

After the labeling pulse, the pH was lowered to 2.5 to quench the H−D exchange reaction by mixing the sample with ~0.5 M HCl. Under these conditions, the refolding reaction was completed. The urea concentrations were kept at 0.82 and 3.0 M throughout the refolding reaction for C121A and A34C/C121A β-lgs, respectively. While the samples of C121A β-lg were treated on ice or at 4 °C after the pH was lowered to pH 2.5, those of A34C/C121A β-lg were incubated for 4 h at 20 °C to complete the refolding reaction.

Then, the samples were concentrated and buffer-exchanged using the same procedures as described above at 4 °C. Finally, concentrated samples containing 3−5 mg/mL β-lg and 10% (v/v) D_2O in ~250 μL were obtained. They were frozen in liquid nitrogen and stored at −80 °C to suppress further H−D exchange reactions until the NMR measurements. The same procedures were used to prepare the reference samples. As the initial reference state without H−D exchange, protonated samples not treated in D_2O were employed. As the final reference state, the samples pulse-labeled 10 min and 4 h after the initiation of refolding were employed for C121A and A34C/C121A β-lgs, respectively.

The NMR measurements were carried out with a DRX 600 instrument at 30 °C. The data obtained were analyzed with Sparky and Igor Pro (WaveMetrics, Lake Oswego, OR). The resultant proton occupancies normalized with the data for the initial and final reference states were fitted to a single-exponential function to extrapolate the duration of the labeling pulse, yielding A_0 values free from the effect of pulse labeling (*36–38*).

Urea Denaturation Monitored by Fluorescence Spectroscopy. Tryptophan fluorescence spectra were measured with an F-7000 fluorescence spectrophotometer (Hitachi, Tokyo, Japan) at 20 °C. Samples contained each protein at 0.1 mg/mL and were prepared in 20 mM glycine-HCl buffer (pH 3.0) with each concentration of urea. The excitation wavelength was 295 nm, and the light path of the cell used was 0.5 cm.

The unfolding curves plotting the fluorescence intensity at 330 nm against the urea concentration, [urea], were analyzed on the basis of the assumption of a two-state transition mechanism and linear dependence of the free energy change of unfolding, ΔG_U, versus [urea] (*39*), as described by the relation

$$\Delta G_U = \Delta G_U^{H_2O} - m[\text{urea}] \quad (2)$$

where $\Delta G_U^{H_2O}$ is the free energy change of unfolding in the absence of urea and m is a measure of the cooperativity of unfolding. The unfolding curves were fitted to the equation with Igor Pro. The midpoint urea concentration of unfolding, C_m, is calculated with the following equation

$$C_m = \Delta G_U^{H_2O}/m \quad (3)$$

Refolding Kinetics Monitored by Fluorescence Spectroscopy with Manual Mixing. Changes in tryptophan fluorescence upon refolding were recorded with an F-7000 fluorescence spectrophotometer at 20 °C. Refolding was initiated by an 8.5-fold dilution with refolding buffer by manual mixing in a tube, and then the sample was transferred into an observation cell. The dead time was ~10 s. Tryptophan residues were excited at 295 nm, and the fluorescence was detected at 330 nm. The resultant kinetic traces were normalized assuming the baselines for the native and denatured states.

Stopped-Flow Measurements. Stopped-flow measurements were performed with a model 400 CD spectrometer at 20 °C. The dead time of mixing was calculated to be 10 ms from the reaction between *N*-acetyl-L-tryptophanamide and *N*-bromosuccinimide. The refolding reactions were monitored by the measuring tryptophan fluorescence excited at 295 nm and detected with a 330 nm band-pass filter (Asahi Spectra, Tokyo, Japan) or by CD at 222 nm. The results shown are the average traces of 10 and 50 times for fluorescence and CD, respectively. For fluorescence measurements, the acquired data were normalized as mentioned above. To calculate the mean residue ellipticity in the stopped-flow CD measurements, the initial protein concentrations in 7.0 M urea were determined from the absorbance as mentioned above. The CD data were represented as the mean residue ellipticity at 222 nm, $[\theta]_{222}$.

Measurements of ANS Binding. ANS binding during refolding was monitored with an F-4500 fluorescence spectrophotometer (Hitachi, Tokyo, Japan) at 20 °C. Each refolding sample contained 10 μM ANS. ANS was excited at 350 nm, and the fluorescence was detected continuously at 485 nm or as spectra from 400 to 600 nm.

Analytical Ultracentrifugation. Sedimentation equilibrium measurements were performed with an Optima XL-I analytical centrifuge (Beckman Coulter, Fullerton, CA) at 20 °C as described previously (*18*).

RESULTS

Disulfide-Linked Dimer of the C121A β-lg Mutant. The structure of A34C/C121A β-lg at pH 3.0 was compared with that of C121A β-lg at pH 3.0 and 6.0 by measuring far- and near-UV CD spectra (Figure 1). The far-UV CD intensity of A34C/C121A β-lg at pH 3.0 is slightly smaller than that of C121A β-lg. However, judging from the similarity of HSQC spectra as described below, the overall contents of the secondary structure of C121A and A34C/C121A β-lgs were similar, although not the same. The near-UV spectrum of A34C/C121A β-lg at pH 3.0 was more similar to that of C121A β-lg at pH 6.0 than that of C121A β-lg at pH 3.0. This indicated that the disulfide-linked A34C/C121A dimer has a structure similar to that of C121A β-lg at pH 6.0, where C121A β-lg assumes the form of a noncovalently linked homodimer.

To analyze the folding mechanisms of the β-lg mutants at the residue level, we measured the $^1H-^{15}N$ HSQC spectra

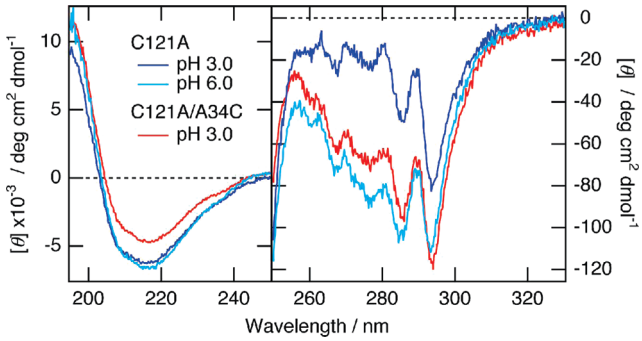

FIGURE 1: CD spectra of the β-lg mutants. Far- and near-UV CD spectra of C121A β-lg at pH 3.0 (blue) or pH 6.0 (cyan) and 20 °C and A34C/C121A β-lg at pH 3.0 (red) and 20 °C.

of C121A β-lg and A34C/C121A β-lg at pH 2.5 (Figure 2). Assignments of the cross-peaks were accomplished on the basis of the ^{15}N-edited TOCSY-HSQC and NOESY-HSQC spectra recorded at 40 °C. Consequently, 97% of the amide cross-peaks of C121A β-lg and A34C/C121A β-lg were assigned. The chemical shifts are listed in Tables S1 and S2 of the Supporting Information. In the pulse labeling measurements, the HSQC spectra were measured at a lower temperature, 30 °C, to suppress further exchange reactions. Thus, the cross-peaks at 30 °C were also assigned on the basis of the TOCSY-HSQC spectra recorded at 30 °C and the chemical shift changes as the temperature decreased from 40 to 30 °C.

Urea Denaturation and Reversibility from the Unfolded State. Urea-induced unfolding was monitored by tryptophan fluorescence. Bovine β-lg has two tryptophan residues, Trp19 and Trp61 (see Figure 6 below). Whereas Trp19 is fully buried inside the β-barrel, Trp61 is exposed to solvent. The spectral change of bovine β-lg upon unfolding is considered to arise mainly from Trp19 because of the weak fluorescence of W19A β-lg (*40*). A34C/C121A β-lg exhibited a similar change in fluorescence to C121A β-lg upon urea unfolding at pH 3.0 (Figure 3a,c), implying that the environment around each tryptophan residue was not affected by the A34C mutation. The apparent $\Delta G_U^{H_2O}$ value of A34C/C121A β-lg obtained from the unfolding experiment was slightly higher than that of C121A β-lg (Figure 3b,d and Table 1). The C_m and m values showed that the disulfide linkage resulted in unfolding at a slightly higher urea concentration with almost the same cooperativity. However, it is possible that the low reversibility of the unfolding of A34C/C121A β-lg under the strongly native conditions affected the unfolding transition curve (see below). Both C121A β-lg and A34C/C121A β-lg were fully denatured in 7.0 M urea at pH 3.0 (Figure 3b,d). These urea and pH conditions were used as the initial unfolding conditions in subsequent experiments.

The reversibility of the unfolding of C121A β-lg and A34C/C121A β-lg was assessed by tryptophan fluorescence and CD spectroscopies. In the fluorescence measurements, when the unfolded samples incubated in 7.0 M urea overnight were refolded in various concentrations of urea diluted 8.5-fold and subsequent overnight incubation, the resultant refolding curves agreed with the unfolding curves (Figure 3b,d). The far- and near-UV CD spectra of A34C/C121A β-lg refolded in 0.82 and 3.0 M urea were also similar to those of the native forms at the respective urea concentrations (data not shown). These results implied that the refolded proteins have secondary and tertiary structures similar to those of the proteins in the native state as monitored using the tryptophan fluorescence and CD spectra.

To examine the reversibility of the unfolding in more detail, the HSQC spectra of the samples after refolding treatment were measured, where the urea in the refolded samples was removed by gel filtration to improve spectral quality. The spectra of C121A β-lg in the native state and after refolding from 7.0 to 0.82 M urea were indistinguishable (Figures 4a and S1a). To our surprise, the spectrum of A34C/C121A β-lg refolded in 0.82 M urea was clearly different from that of the native A34C/C121A β-lg (Figures 4b and S1b). Large shifts, signal broadening, and/or signal splits were observed for many peaks, revealing that the reversibility of A34C/C121A β-lg was, in fact, quite low in 0.82 M urea.

To improve the reversibility of A34C/C121A β-lg, we examined various refolding conditions, i.e., lower and higher temperatures (5 and 50 °C, respectively), neutral pH (pH 6.0), and lower and higher urea concentrations (0.07 and 3.5 M, respectively). We found that refolding in 3.0 or 3.5 M urea rather than 0.82 M gave an NMR spectrum much higher in quality (Figures 4c and S1c). The dependence of one-dimensional (1D) ^{1}H NMR spectra on the urea concentration showed that the lower the urea concentration, the lower the reversibility (Figure S2a). This is contrary to our expectation that the strongly native conditions should promote efficient refolding. It should be noted that, when these 1D ^{1}H NMR measurements were made, the urea concentrations were adjusted to 0.82 M to measure the spectra under the same conditions among various samples. In the HSQC spectrum of the A34C/C121A β-lg refolded in 3.0 M urea (Figures 4c and S1c), although some peaks still appeared at positions different from the native state, the signals became much sharper and more similar to those of the native A34C/C121A β-lg, in comparison with the spectrum for the sample directly refolded in 0.82 M urea (Figures 4b and S1b). Moreover, the spectrum of the sample incubated in 3.0 M urea for 6 h after the direct refolding treatment in 0.82 M urea was indistinguishable from that of the sample directly refolded in 3.0 M urea, escaping from the misfolded state (data not shown). The chemical shift differences between the native sample and the sample refolded in 3.0 M urea are plotted in Figure S2b. The residues with relatively large differences were located in the loops between the β-strands, D and E strands, and α-helix. Although the HSQC spectra still exhibited small differences between the native sample and the sample refolded in 3.0 M, the refolding conditions from 7.0 to 3.0 M urea were used in the subsequent refolding experiments with A34C/C121A β-lg.

To examine whether the low reversibility of the unfolded A34C/C121A β-lg was caused by the generation of higher-order oligomers, sedimentation equilibrium experiments were performed. However, no oligomer other than a dimer was detected in the samples refolded in 0.82 and 3.0 M urea or the native sample (Table 2). These results suggest that the low reversibility stems from the non-native interactions produced within each disulfide-linked dimer.

Refolding Kinetics Monitored by Fluorescence and CD. Refolding kinetics was monitored using tryptophan fluorescence with manual and stopped-flow mixing for both the C121A and A34C/C121A mutants. With the manual mixing in 0.82 M urea, C121A β-lg exhibited a small increase in

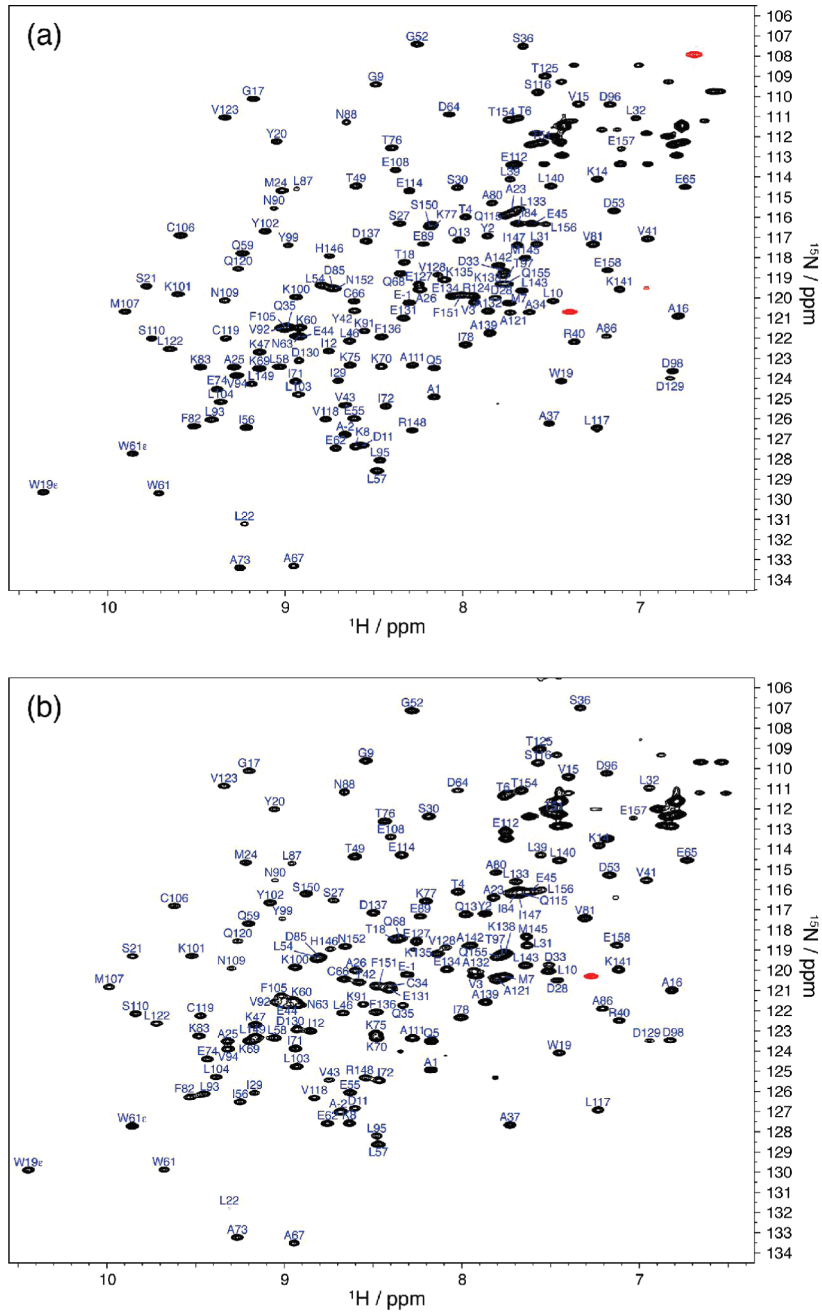

FIGURE 2: ^{1}H−^{15}N HSQC spectra of C121A β-lg (a) and A34C/C121A β-lg (b) at pH 2.5 and 40 °C. The labels indicate the assignments of the cross-peaks corresponding to the backbone H^N−N cross-peak or the side chain H^ε−N^ε cross-peak of tryptophan residues. The red peaks are those with negative intensities. The spectra were rendered with NMRDraw (*34*).

fluorescence at 330 nm, which could be fitted with a single-exponential function (Figure 5b). With the stopped-flow mixing monitored at 330 nm, a larger change in fluorescence with the conversion of the unfolded form to the native structure was observed (Figure 5a). The kinetic trace was fitted with a quadruple-exponential function. The kinetic parameters are listed in Table 3. These parameters are consistent with those reported for wild-type β-lg (*28*). The last of the four phases corresponds to that observed in the manual mixing experiment.

In contrast, the refolding reaction of A34C/C121A β-lg in 3.0 M urea monitored with the stopped-flow equipment could not be fitted well because of the slow kinetics and small change in amplitude (Figure 5a). However, a notable burst-phase amplitude was observed, indicating that a structured burst-phase intermediate was formed within the dead time of stopped-flow mixing, 10 ms. As for the manual mixing experiment in 3.0 M urea, the kinetic trace was fitted with a double-exponential function (Figure 5b and Table 3). We also performed the kinetic fluorescence measurements in 0.82 M urea. The overall kinetics was faster in 0.82 M urea than in 3.0 M urea (Figure 5b and Table 3).

Stopped-flow CD experiments were carried out to assess the extent to which non-native α-helices formed in the folding intermediates. Within the dead time of 10 ms, C121A β-lg in 0.82 M urea showed an overshoot indicating the accumulation of intermediates with non-native α-helices (Figure 5c) as observed for wild-type β-lg (*22, 28*). As for A34C/C121A β-lg, only a slight overshoot appeared in the kinetic trace of the refolding from 7.0 to 3.0 M urea

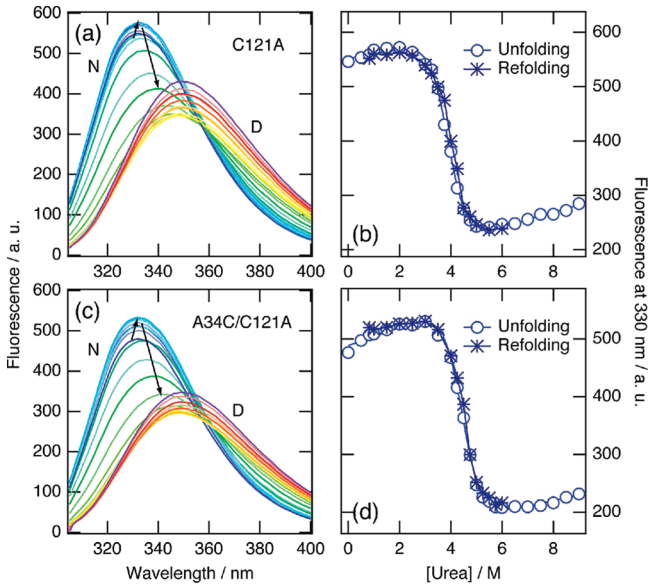

FIGURE 3: Urea-induced unfolding and refolding transitions of the β-lg mutants at pH 3.0 and 20 °C. (a and c) Changes in tryptophan fluorescence of C121A (a) and A34C/C121A (c) β-lgs upon unfolding from 0 to 9.0 M urea. Arrows indicate the directions of the changes with the increase in urea concentration. (b and d) Comparison of the unfolding curves (○) and refolding curves (∗) of C121A β-lg (b) and A34C/C121A β-lg (d) obtained by plotting fluorescence intensity at 330 nm vs urea concentration.

Table 1: Thermodynamic Parameters for the β-lg Mutants at pH 3.0 and 20 °C[a]

species	where $\Delta G_U^{H_2O}$ (kJ/mol)	m (kJ mol^{-1} M^{-1})	C_m (M)
C121A	27.1 ± 1.3	7.0 ± 0.3	3.9
A34C/C121A	29.7 ± 1.6	6.7 ± 0.3	4.4

[a] Errors are fitting errors.

(Figure 5c). To examine the effects of urea, the experiments were performed at different concentrations of urea. The amplitude of overshoot for C121A β-lg was smaller in 2.0 M urea than in 0.82 M urea (data not shown). Consistently, the amplitude of overshoot for A34C/C121A β-lg was smaller in 3.0 M urea than in 0.82 M urea (Figure 5c). Although the low reversibility in 0.82 M urea makes a fair assessment of the formation of non-native α-helices difficult, it can be assumed that the increase in the concentration of urea leads to less accumulation of non-native α-helices and that A34C/C121A β-lg also forms non-native α-helices to the same extent as C121A β-lg.

To assess the exposure of hydrophobic surfaces during refolding, 1-anilinonaphthalene-8-sulfonic acid (ANS) binding experiments were carried out (Figure 5d−f). When the refolding of C121A β-lg was initiated with manual mixing in the presence of 10 μM ANS and 0.82 M urea, the ANS fluorescence increased rapidly within the dead time and then decreased slowly to the level for the native C121A β-lg (Figure 5d). The rate of decrease was close to that of the slowest phase monitored with tryptophan fluorescence (Table 3). This indicates that the intermediates of C121A β-lg bind ANS molecules to the exposed hydrophobic regions and release them upon formation of the native protein (Figure 5d,e). In the case of A34C/C121A β-lg refolded in 0.82 M urea, although a similar transient increase in ANS fluorescence was observed, the level of fluorescence did not reach that of the native form (Figure 5d,f), indicating that A34C/C121A β-lg was trapped in the non-native state with significant hydrophobic regions exposed. In the presence of 3.0 M urea, the extent of the transient increase in ANS fluorescence was smaller, and moreover, the spectrum after refolding agreed with that of the native A34C β-lg in 3.0 M urea (Figure 5d,f). Since a decrease in fluorescence in 2.0 M urea was also observed for C121A β-lg (data not shown), the decrease represents common effects of urea on the refolding intermediates. On the other hand, the final level of ANS fluorescence confirmed that, in 0.82 M urea, while C121A β-lg refolded mostly into the native structure, A34C/C121A β-lg did not and that, in 3.0 M urea, the refolding yield of A34C/C121A β-lg increased significantly.

H−D Exchange Pulse Labeling. H−D exchange pulse labeling combined with NMR analysis was employed to obtain structural information about the intermediates that accumulated within 10 ms. These intermediates exhibited burst-phase amplitudes in the stopped-flow fluorescence experiments and overshoots in the stopped-flow CD experiments. In this study, we performed several experiments in which the duration of the labeling pulse was changed. Then, by extrapolating the duration time to zero with a single-exponential function, we calculated A_0, the proton occupancy value free from the effect of the labeling pulse (*36–38*). However, for some residues, proton occupancy depended little upon the duration of labeling pulse, making the fitting difficult. For such residues, average values were used instead of extrapolated values. Furthermore, the residues showing little difference between references 1 and 0 were not used as probes (Figure S3).

The number of probes available for C121A β-lg refolded in 0.82 M urea and A34C/C121A β-lg refolded in 3.0 M urea was 69, including one for a side chain, and 46, respectively (Figures 6a,b and S4). In the plots, an A_0 of 0 means that the amide proton was completely protected from exchange and an A_0 of 1 no protection. In other words, the lower the value of A_0, the more structured the residue is at a refolding time of 10 ms. The intermediate of C121A β-lg at 10 ms had several structured regions where relatively low and similar A_0 values are contiguous in the primary sequence (Figure 6a,c). Such regions are the B, C, F, G, and H β-strands and the loop region after the main α-helix.

In the experiments with A34C/C121A β-lg, because of the slow refolding kinetics, the refolding time after pulse labeling was set to 4 h, which is much longer than that of C121A β-lg, i.e., 10 min. The H−D exchange reactions occurring during the long refolding time affected the quality of the data. Nevertheless, we can conclude that the structured regions in the burst-phase intermediate of A34C/C121A β-lg were similar to those of C121A β-lg (Figure 6b,d). These regions are rich in hydrophobic residues, suggesting the rapid formation of nativelike hydrophobic cores. The hydrophobic residues may interact rapidly within a relatively small space without being affected by other peripheral residues, leading to the fast formation of the core β-sheets in the monomer or dimer.

DISCUSSION

Kinetic Trapping of the Disulfide-Linked β-lg Dimer. Although the native forms of C121A β-lg and A34C/C121A β-lg are similar in structure, A34C/C121A β-lg exhibited

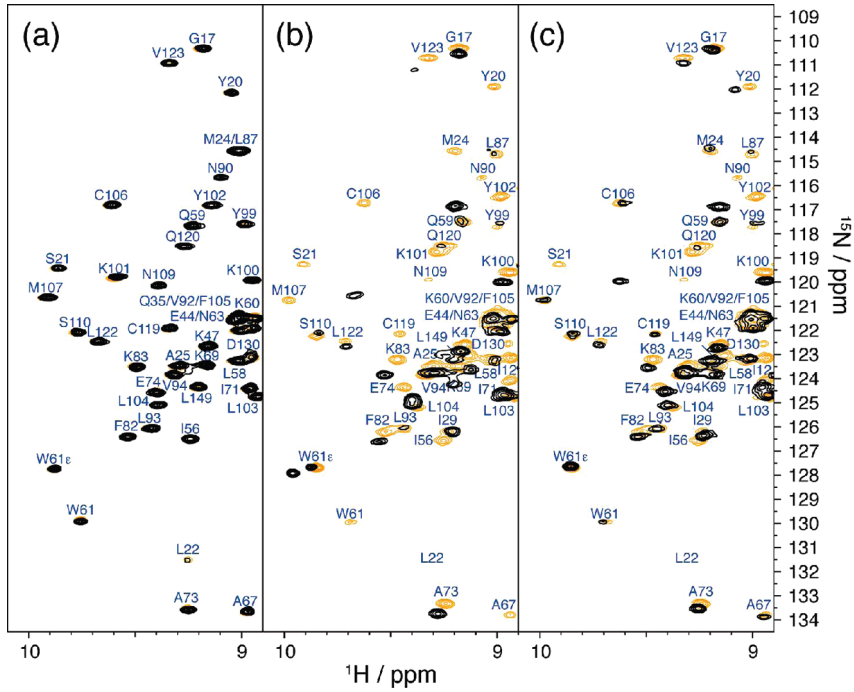

FIGURE 4: Parts of the ^{1}H−^{15}N HSQC spectra of the native (orange) and refolded (black) forms of the β-lg mutants measured at pH 2.5 and 30 °C. The samples were refolded from 7.0 to 0.82 M urea for C121A β-lg (a) and 0.82 M (b) or 3.0 M (c) urea for A34C/C121A β-lg at pH 3.0 and 20 °C. The spectra were rendered with NMRDraw (*34*). The full spectra are shown in Figures 2 and S1.

Table 2: Apparent Molecular Weights of the Native and Refolded A34C/C121A β-lgs in 3.0 and 0.82 M Urea[a]

concentration	M_{app} (native)	M_{app} (7.0 → 3.0 M)	M_{app} (7.0 → 0.82 M)
0.3 mg/mL	3.4×10^4	3.5×10^4	3.6×10^4
0.6 mg/mL	3.4×10^4	3.3×10^4	3.4×10^4
0.9 mg/mL	3.2×10^4	3.5×10^4	3.6×10^4

[a] The apparent molecular weights were calculated from the sedimentation equilibrium analyses at pH 3.0 and 20 °C.

remarkably slow refolding kinetics, and the reversibility in 0.82 M urea was obviously low according to the results of the NMR measurements (Figures 4 and S1). The ANS binding experiments indicated that the A34C/C121A β-lg which refolded in 0.82 M urea was trapped in a form with more hydrophobic regions exposed than the native species (Figure 5d−f). However, the trapped species could not be distinguished from the native one when monitored using tryptophan fluorescence spectroscopy (Figure 3) and far- and near-UV CD spectra (data not shown). These results indicate that the trapped species has a secondary and tertiary structure similar to that of the native species, although the precise conformation differed with more hydrophobic regions exposed.

In 3.0 M urea, the reversibility was much higher judging from the NMR and ANS fluorescence spectra (Figures 4 and 5d−f). This indicates that the strongly native conditions achieved with 0.82 M urea adversely affect the refolding to the native structure. Importantly, the trapped species formed in 0.82 M could be rescued by subsequent incubation in 3.0 M urea for 6 h, regenerating the mostly native species. Sedimentation equilibrium experiments revealed that the samples refolded in 0.82 M and 3.0 M urea did not form oligomers larger than a dimer (Table 2). These results argue that the strong non-native intra- and intermonomer interactions exerted at a low urea concentration (i.e., strongly native conditions) trapped the misfolded dimers in a glassy state in which molecular conformations are frozen and thermodynamically isolated from one another. In other words, under the strongly native conditions, the misfolded dimers would be separated from the native dimers by a high energy barrier (Figure 7). On the other hand, at moderate urea concentrations (i.e., mildly native conditions), non-native interactions are less stabilized and, at the same time, the energy barriers are lower, so the trapped species can be annealed to the native species.

Folding Mechanism of the Disulfide-Linked β-lg Dimer. In spite of the slow refolding of A34C/C121A β-lg in 0.82 and 3.0 M urea, notable changes in fluorescence occurred within the dead time of the stopped-flow mixing, 10 ms (Figure 5a). Also in the stopped-flow CD experiments, within 10 ms, a significant amount of secondary structure was formed (Figure 5c). The burst-phase non-native α-helices were also formed as was the case for wild-type β-lg, although the magnitude depended on the concentration of urea: the burst-phase amplitude was lower at higher urea concentrations. The H−D exchange pulse labeling measurements suggested that the structured regions of A34C/C121A β-lg during the burst phase in 3.0 M urea are similar to those of the monomeric C121A β-lg, i.e., the B, C, F, G, and H β-strands. Although the strong protection of G and H strands as shown in Figure 6 was similarly observed in our previous reports with wild-type β-lg (*27, 28*), the protection pattern of other regions was distinct. Kuwata et al. (*28*) have suggested the protection of A, F, G, and H strands and the main α-helix at an early stage of the refolding, within 1.8 ms, and the existence of non-native α-helix around strand A. Considering that Kuwata et al. (*28*) observed drastic change in proton occupancy within 10 ms, this difference may be caused by the limitation of our apparatus with a dead time of 10 ms. It is likely that there are large differences between the structures at 1.8 and 10 ms. Another possibility is that the distinct pattern of protections is caused by the

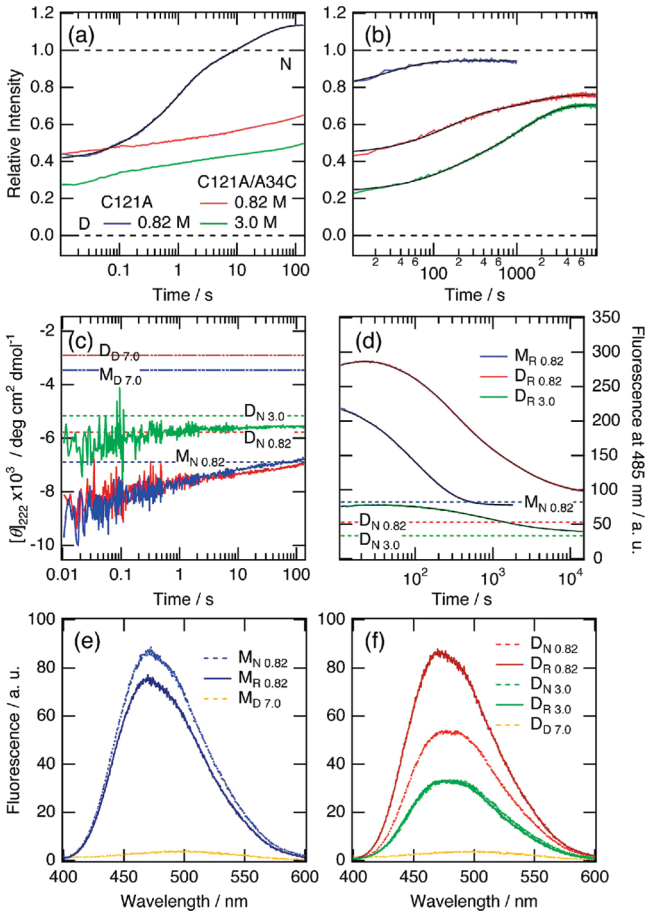

FIGURE 5: Refolding kinetics of the β-lg mutants. Refolding kinetic traces of C121A β-lg from 7.0 to 0.82 M urea (blue) and A34C/C121A β-lg from 7.0 to 0.82 M (red) or 3.0 M (green) urea by manual (b) and stopped-flow (a and c) mixing monitored using tryptophan fluorescence at 330 nm (a and b) and CD at 222 nm (c) at pH 3.0 and 20 °C. (a and b) Tryptophan fluorescence intensity was normalized assuming the levels of the native (N) and denatured (D) forms. The fitting curves are colored black. (c) The subscripts N0.82, N3.0, and D7.0 with *M* and *D* denote the levels of the native forms in 0.82 and 3.0 M urea and the denatured forms in 7.0 M urea of C121A β-lg (*M*, monomer) and A34C/C121A β-lg (*D*, dimer), respectively. (d) Refolding kinetic traces of C121A β-lg from 7.0 to 0.82 M urea ($M_{R0.82}$) and A34C/C121A β-lg from 7.0 to 0.82 M ($D_{R0.82}$) or 3.0 M ($D_{R3.0}$) urea monitored by measuring ANS fluorescence at 485 nm, pH 3.0, and 20 °C. $M_{N0.82}$, $D_{N0.82}$, and $D_{N3.0}$ denote the levels of the native forms of C121A β-lg in 0.82 M urea and A34C/C121A β-lg in 0.82 and 3.0 M urea, respectively. The fitting curves are colored black. (e and f) ANS fluorescence spectra of C121A β-lg (*M*) (e) and A34C/C121A β-lg (*D*) (f) in the native state and the refolded state in 0.82 M (N0.82 and R0.82) or 3.0 M (N3.0 and R3.0) urea and the denatured state in 7.0 M urea (D7.0).

difference in the pulse labeling methods employed. In this study, by extrapolating the length of pulse labeling to time zero, we calculated the A_0 value free from the effects of pulse labeling. On the other hand, Kuwata et al. (*28*) calculated the protection factors by changing the pH of pulse labeling. Additionally, because the counterpart of the main α-helix, Cys121 on strand H, was mutated in C121A β-lg, the formation of the main α-helix might be affected. Recently, Nakagawa et al. (*41*) have suggested the existence of non-native α-helix around strand H in the acid-induced equilibrium intermediate of equine β-lg. However, at this moment, it is difficult to compare their results with ours because the two β-lgs from different species exhibit various structural differences. Most importantly, bovine β-lg retains the native conformation at acidic pH where equine β-lg assumes the intermediate state.

Taking into account the results described above, we suggest why the refolding of A34C/C121A β-lg is so slow in comparison with the refolding of C121A β-lg. For both C121A β-lg and A34C/C121A β-lg, regions including the B, C, F, G, and H β-strands rich in hydrophobic residues form nativelike core structures rapidly within 10 ms, mainly via local hydrophobic interactions. In addition, non-native α-helices are formed in several regions. As for C121A β-lg, the subsequent slow kinetics after the burst phase arise from a rearrangement of the non-native α-helices into the native β-strands and concomitant formation of the specific side chain interactions. These events occur intramolecularly.

In the case of A34C/C121A β-lg, we found that a similar burst-phase intermediate with core β-strands and non-native α-helices is formed. The core structure is mainly formed by local hydrophobic interactions independent of molecular size and redundant sequence. Although a considerable amount of secondary and tertiary structure is formed in the intermediate, additional non-native intermonomer interactions are likely to be formed in the burst and subsequent phases. In the presence of 3.0 M urea, although these non-native interactions slow the refolding, A34C/C121A β-lg manages to refold to the native structure, jumping over the kinetic high energy barriers. However, in 0.82 M urea, wrong interactions are too stable to rearrange into the native forms, so the molecules are trapped (i.e., frozen) in the misfolded glassy state with an exposed hydrophobic surface. This results in the low reversibility observed under strongly native conditions (Figure 7).

To discuss further the effects of increasing size on protein folding, it is significant to compare our results with those on the folding kinetics of engineered chymotrypsin inhibitor 2 (CI2) (*42*). Inaba et al. (*42*) conducted the kinetic experiments using the double-CI2 protein, in which another CI2 polypeptide was inserted into the loop region of the parent CI2. In both their and our studies, the doubled proteins folded much slower than the monomeric proteins. Intriguingly, double CI2 folded into two distinct native conformations as revealed by twin peaks of HSQC spectra. In the case of A34C/C121A β-lg, twin peaks were apparently observed for the side chain of Trp61 in the HSQC spectrum when the protein was refolded in 0.82 M urea (Figure 4b). However, peaks from some residues became broad compared to those in the native state, suggesting that some regions of the refolded A34C/C121A β-lg had multiple conformations. When the results from the different techniques are combined, we find that the trapped glassy states might be a mixture of several species, in which some residues adopt unique conformations similar to those of the native state, giving relatively sharp peaks in the HSQC spectra and the similarity of overall secondary structure.

When the protein molecules are large, the refolding yield decreases seriously, leading to irreversible unfolding even for proteins made up of domains. Here, the folding of the disulfide-linked dimer of β-lg illustrates how the efficiency of the refolding process is determined by an energetic balance of correct and incorrect interactions. The refolding reaction of β-lg, a β-barrel protein made of 162 amino acid residues, is intrinsically complicated, experiencing an α-helix−β-sheet

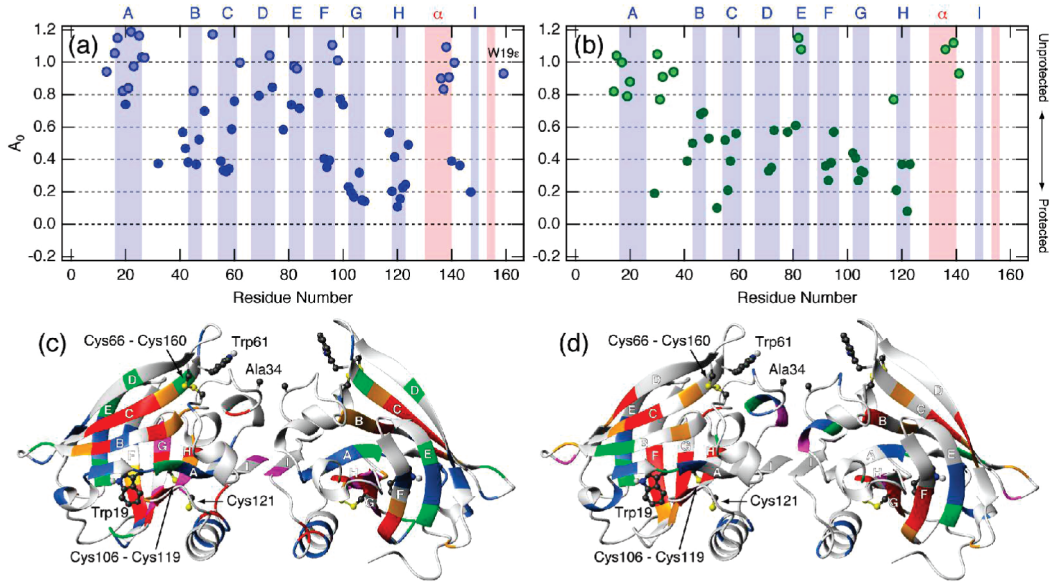

FIGURE 6: H−D exchange pulse labeling of the β-lg mutants. (a and b) The A_0 values of C121A β-lg (a) and A34C/C121A β-lg (b) extrapolated (●) and averaged (○) with proton occupancies for the various pulse labeling durations at a refolding time of 10 ms. Letters A−I and α and the corresponding colored regions represent the secondary structures in β-lg. (c and d) Mapping of the structured region of C121A β-lg (c) and A34C/C121A β-lg (d) on the crystal structure of the wild-type β-lg dimer. The colors correspond to the A_0 values shown in panels a and b: pink for <0.2, red for 0.2−0.4, orange for 0.4−0.6, green for 0.6−0.8, and blue for >0.8. The side chains are indicated for Ala34, Cys121, Trp19, Trp61, and disulfide bonds (Cys66−Cys160 and Cys106−Cys119). The structure was rendered with MolMol (*44*) from the coordinate data of Protein Data Bank entry 1BEB (*8*).

Table 3: Kinetic Parameters of the Refolding Reactions of β-lg Mutants at pH 3.0 and 20 °C[a]

C121A

type of mixing		burst phase	k_1 (s^{-1})	k_2 (s^{-1})	k_3 (s^{-1})	k_4 (s^{-1})	k_5 (s^{-1})
7.0 → 0.82 M urea	stopped-flow (Trp)	− (41%)	9.1 ± 0.4 (8%)	1.1 (35%)	(2.5 ± 0.3) × 10^{-1} (11%)	(4.4 ± 0.1) × 10^{-2} (19%)	−
	manual (Trp)	− (79%)	−	−	−	(3.2 ± 0.2) × 10^{-2} (15%)	−
	manual (ANS)	−	−	−	−	1.7 × 10^{-2} (40%)	6.1 × 10^{-3} (60%)

A34C/C121A

type of mixing		burst phase	k_1 (s^{-1})	k_2 (s^{-1})	k_3 (s^{-1})	k_4 (s^{-1})
7.0 → 0.82 M urea	manual (Trp)	− (44%)	−	(7.4 ± 0.2) × 10^{-3} (20%)	(7.5 ± 0.1) × 10^{-4} (12%)	−
	manual (ANS)	−	1.3 × 10^{-1} (22%[b])	3.9 × 10^{-3} (39%[b])	(8.1 ± 0.1) × 10^{-4} (24%[b])	2.0 × 10^{-4} (16%[b])
7.0 → 3.0 M urea	manual (Trp)	− (24%)	−	(7.1 ± 0.3) × 10^{-3} (13%)	8.3 × 10^{-4} (34%)	−
	manual (ANS)	−	(8.6 ± 0.5) × 10^{-2} (19%[b])	(3.8 ± 0.1) × 10^{-3} (16%[b])	(9.0 ± 0.1) × 10^{-4} (46%[b])	1.6 × 10^{-4} (20%[b])

[a] Errors are fitting errors. [b] Negative amplitudes after the overshoot.

transition. Doubling the size by introducing the intermolecular disulfide bridge increases the chance of wrong intermolecular interactions, such as possible domain swapping caused by redundant sequence, particularly during folding. Nevertheless, the folding core is rapidly formed within milliseconds mainly by local hydrophobic interactions inside each domain. In the subsequent folding steps, unless the wrong intermolecular interactions are highly stable, the β-lg dimer refolds successfully to form the native structure, even though folding rates are seriously reduced. However, if the interactions are too strong, non-native conformations are frozen as observed here, forming the glasslike misfolded species.

CONCLUSIONS

A disulfide-linked dimer of β-lg without the free thiol group, A34C/C121A β-lg, was constructed to investigate the folding mechanism of a large protein in which many components interact in a small space. The refolding of a disulfide-linked dimer of A34C/C121A β-lg was very slow in comparison with that of the monomeric C121A β-lg, and the reversibility was not complete. The refolding yield depended on the urea concentration: the lower the concentration, the lower the yield. A comparison of the burst-phase intermediates of the monomeric C121A β-lg and dimeric A34C/C121A β-lg indicated that the core β-strands which formed early in the refolding process are similar to each other. The results suggest that the non-native interactions between the monomers occur through peripheral residues, i.e., exposed loops and noncore residues, in A34C/C121A β-lg. The intermediates can slowly transform into the native structure unless the stability of the non-native interactions is high. However, under strongly native conditions, these

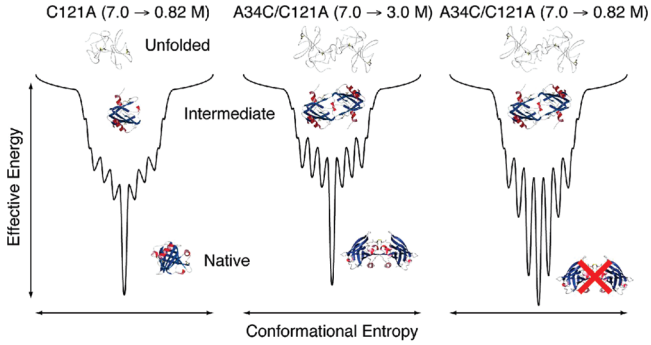

FIGURE 7: Schematic representation of the folding mechanisms of the β-lg mutants using the folding funnels. At the early stage of refolding, the β-lg mutants fold similarly, driven by hydrophobic interactions. In the following steps, while the monomeric β-lg folds as smoothly as wild-type β-lg, the disulfide-linked dimeric β-lg folds much more slowly due to many non-native interactions causing the rough funnel surface. Unless the non-native interactions are destabilized by moderate concentrations of denaturant, making the funnel surface smoother, the dimeric β-lg remains in a glasslike trapped state.

non-native interactions are stabilized, leading to the glassy trapped state.

The picture of refolding of A34C/C121A β-lg described above is in agreement with the concept of a funnel-like folding landscape (Figure 7): overly strong interactions make the folding funnel rough, producing many kinetic traps which prevent efficient and rapid folding (*4, 43*). These results also suggest that many large proteins can refold by taking advantage of a mechanism similar to that observed for the refolding of A34C/C121A β-lg in 3.0 M urea. In other words, for large proteins, kinetic trapping by non-native interactions would be inevitable. One approach to preventing such kinetic trapping is, as demonstrated here, to destabilize the native form, which has the simultaneous effect of melting the frozen glasslike intermediate. This approach is a technologically important way to enhance the yield of refolding from the denatured proteins, e.g., inclusion bodies. An alternative approach might be a unique folding pathway evading the kinetic traps, instead of multiple folding pathways as suggested by the folding funnel.

SUPPORTING INFORMATION AVAILABLE

NMR spectra and analyzed data (Figures S1−S4) and chemical shift tables (Tables S1 and S2). This material is available free of charge via the Internet at http://pubs.acs.org.

REFERENCES

1. Wolynes, P. G., Onuchic, J. N., and Thirumalai, D. (1995) Navigating the folding routes. *Science 267*, 1619–1620.
2. Dobson, C. M., and Karplus, M. (1999) The fundamentals of protein folding: Bringing together theory and experiment. *Curr. Opin. Struct. Biol. 9*, 92–101.
3. Dinner, A. R., Sali, A., Smith, L. J., Dobson, C. M., and Karplus, M. (2000) Understanding protein folding via free-energy surfaces from theory and experiment. *Trends Biochem. Sci. 25*, 331–339.
4. Wolynes, P. G. (2005) Energy landscapes and solved protein-folding problems. *Philos. Trans. R. Soc. London, Ser. A 363*, 453–464.
5. Fersht, A. R. (2000) Transition-state structure as a unifying basis in protein-folding mechanisms: Contact order, chain topology, stability, and the extended nucleus mechanism. *Proc. Natl. Acad. Sci. U.S.A. 97*, 1525–1529.
6. Dill, K. A., and Chan, H. S. (1997) From Levinthal to pathways to funnels. *Nat. Struct. Biol. 4*, 10–19.
7. Mi, D., Kim, H. J., Hadziselimovic, A., and Sanders, C. R. (2006) Irreversible misfolding of diacylglycerol kinase is independent of aggregation and occurs prior to trimerization and membrane association. *Biochemistry 45*, 10072–10084.
8. Brownlow, S., Morais Cabral, J. H., Cooper, R., Flower, D. R., Yewdall, S. J., Polikarpov, I., North, A. C., and Sawyer, L. (1997) Bovine β-lactoglobulin at 1.8 Å resolution—Still an enigmatic lipocalin. *Structure 5*, 481–495.
9. Hambling, S. G., MacAlpine, A. S., and Sawyer, L. (1992) *β-Lactoglobulin*, Elsevier, Amsterdam.
10. Kontopidis, G., Holt, C., and Sawyer, L. (2002) The ligand-binding site of bovine β-lactoglobulin: Evidence for a function? *J. Mol. Biol. 318*, 1043–1055.
11. Qin, B. Y., Bewley, M. C., Creamer, L. K., Baker, H. M., Baker, E. N., and Jameson, G. B. (1998) Structural basis of the Tanford transition of bovine β-lactoglobulin. *Biochemistry 37*, 14014–14023.
12. Qin, B. Y., Creamer, L. K., Baker, E. N., and Jameson, G. B. (1998) 12-Bromododecanoic acid binds inside the calyx of bovine β-lactoglobulin. *FEBS Lett. 438*, 272–278.
13. Sawyer, L., and Kontopidis, G. (2000) The core lipocalin, bovine β-lactoglobulin. *Biochim. Biophys. Acta 1482*, 136–148.
14. Uhrín´ová, S., Smith, M. H., Jameson, G. B., Uhrín´, D., Sawyer, L., and Barlow, P. N. (2000) Structural changes accompanying pH-induced dissociation of the β-lactoglobulin dimer. *Biochemistry 39*, 3565–3574.
15. Kuwata, K., Hoshino, M., Era, S., Batt, C. A., and Goto, Y. (1998) α → β transition of β-lactoglobulin as evidenced by heteronuclear NMR. *J. Mol. Biol. 283*, 731–739.
16. Kuwata, K., Hoshino, M., Forge, V., Era, S., Batt, C. A., and Goto, Y. (1999) Solution structure and dynamics of bovine β-lactoglobulin A. *Protein Sci. 8*, 2541–2545.
17. Sakai, K., Sakurai, K., Sakai, M., Hoshino, M., and Goto, Y. (2000) Conformation and stability of thiol-modified bovine β-lactoglobulin. *Protein Sci. 9*, 1719–1729.
18. Sakurai, K., and Goto, Y. (2002) Manipulating monomer-dimer equilibrium of bovine β-lactoglobulin by amino acid substitution. *J. Biol. Chem. 277*, 25735–25740.
19. Sakurai, K., Oobatake, M., and Goto, Y. (2001) Salt-dependent monomer-dimer equilibrium of bovine β-lactoglobulin at pH 3. *Protein Sci. 10*, 2325–2335.
20. Hamada, D., Kuroda, Y., Tanaka, T., and Goto, Y. (1995) High helical propensity of the peptide fragments derived from β-lactoglobulin, a predominantly β-sheet protein. *J. Mol. Biol. 254*, 737–746.
21. Kuroda, Y., Hamada, D., Tanaka, T., and Goto, Y. (1996) High helicity of peptide fragments corresponding to β-strand regions of β-lactoglobulin observed by 2D-NMR spectroscopy. *Folding Des. 1*, 255–263.
22. Hamada, D., Segawa, S., and Goto, Y. (1996) Non-native α-helical intermediate in the refolding of β-lactoglobulin, a predominantly β-sheet protein. *Nat. Struct. Biol. 3*, 868–873.
23. Hamada, D., and Goto, Y. (1997) The equilibrium intermediate of β-lactoglobulin with non-native α-helical structure. *J. Mol. Biol. 269*, 479–487.
24. Cohen, F. E. (1999) Protein misfolding and prion diseases. *J. Mol. Biol. 293*, 313–320.
25. Uversky, V. N., and Fink, A. L. (2004) Conformational constraints for amyloid fibrillation: The importance of being unfolded. *Biochim. Biophys. Acta 1698*, 131–153.
26. Krishna, M. M., Hoang, L., Lin, Y., and Englander, S. W. (2004) Hydrogen exchange methods to study protein folding. *Methods 34*, 51–64.
27. Forge, V., Hoshino, M., Kuwata, K., Arai, M., Kuwajima, K., Batt, C. A., and Goto, Y. (2000) Is folding of β-lactoglobulin non-hierarchic? Intermediate with native-like β-sheet and non-native α-helix. *J. Mol. Biol. 296*, 1039–1051.
28. Kuwata, K., Shastry, R., Cheng, H., Hoshino, M., Batt, C. A., Goto, Y., and Roder, H. (2001) Structural and kinetic characterization of early folding events in β-lactoglobulin. *Nat. Struct. Biol. 8*, 151–155.
29. Sakurai, K., and Goto, Y. (2006) Dynamics and mechanism of the Tanford transition of bovine β-lactoglobulin studied using heteronuclear NMR spectroscopy. *J. Mol. Biol. 356*, 483–496.
30. Sakurai, K., and Goto, Y. (2007) Principal component analysis of the pH-dependent conformational transitions of bovine β-lactoglobulin monitored by heteronuclear NMR. *Proc. Natl. Acad. Sci. U.S.A. 104*, 15346–15351.

31. Yagi, M., Sakurai, K., Kalidas, C., Batt, C. A., and Goto, Y. (2003) Reversible unfolding of bovine β-lactoglobulin mutants without a free thiol group. *J. Biol. Chem. 278*, 47009–47015.
32. Kim, T. R., Goto, Y., Hirota, N., Kuwata, K., Denton, H., Wu, S. Y., Sawyer, L., and Batt, C. A. (1997) High-level expression of bovine β-lactoglobulin in *Pichia pastoris* and characterization of its physical properties. *Protein Eng. 10*, 1339–1345.
33. Gill, S. C., and von Hippel, P. H. (1989) Calculation of protein extinction coefficients from amino acid sequence data. *Anal. Biochem. 182*, 319–326.
34. Delaglio, F., Grzesiek, S., Vuister, G. W., Zhu, G., Pfeifer, J., and Bax, A. (1995) NMRPipe: A multidimensional spectral processing system based on UNIX pipes. *J. Biomol. NMR 6*, 277–293.
35. Goddard, T. D., and Kneller, D. G. (2003) SPARKY 3, University of California, San Francisco.
36. Nishimura, C., Dyson, H. J., and Wright, P. E. (2002) The apomyoglobin folding pathway revisited: Structural heterogeneity in the kinetic burst phase intermediate. *J. Mol. Biol. 322*, 483–489.
37. Nishimura, C., Dyson, H. J., and Wright, P. E. (2006) Identification of native and non-native structure in kinetic folding intermediates of apomyoglobin. *J. Mol. Biol. 355*, 139–156.
38. Nishimura, C., Wright, P. E., and Dyson, H. J. (2003) Role of the B helix in early folding events in apomyoglobin: Evidence from site-directed mutagenesis for native-like long range interactions. *J. Mol. Biol. 334*, 293–307.
39. Pace, C. N. (1990) Conformational stability of globular proteins. *Trends Biochem. Sci. 15*, 14–17.
40. Cho, Y., Batt, C. A., and Sawyer, L. (1994) Probing the retinol-binding site of bovine β-lactoglobulin. *J. Biol. Chem. 269*, 11102–11107.
41. Nakagawa, K., Tokushima, A., Fujiwara, K., and Ikeguchi, M. (2006) Proline scanning mutagenesis reveals non-native fold in the molten globule state of equine β-lactoglobulin. *Biochemistry 45*, 15468–15473.
42. Inaba, K., Kobayashi, N., and Fersht, A. R. (2000) Conversion of two-state to multi-state folding kinetics on fusion of two protein foldons. *J. Mol. Biol. 302*, 219–233.
43. Socci, N. D., Onuchic, J. N., and Wolynes, P. G. (1998) Protein folding mechanisms and the multidimensional folding funnel. *Proteins 32*, 136–158.
44. Koradi, R., Billeter, M., and Wuthrich, K. (1996) MOLMOL: A program for display and analysis of macromolecular structures. *J. Mol. Graphics 14*, 29–32, 51−55.

BI8001715